


RESEARCH ARTICLE OPEN ACCESS

Serinc5 Regulates Sequential Chondrocyte Differentiation by Inhibiting Sox9 Function in Pre-Hypertrophic Chondrocytes

Kenji Hata¹  | Kanta Wakamori^{1,2} | Akane Hirakawa-Yamamura^{1,3} | Sachi Ichiyama-Kobayashi^{1,2} | Masaya Yamaguchi^{4,5,6} | Daisuke Okuzaki⁷ | Yoshifumi Takahata^{1,8} | Tomohiko Murakami¹ | Narikazu Uzawa² | Takashi Yamashiro³ | Riko Nishimura¹

¹Department of Molecular and Cellular Biochemistry, Osaka University Graduate School of Dentistry, Osaka, Japan | ²Department of Oral & Maxillofacial Oncology and Surgery, Osaka University Graduate School of Dentistry, Osaka, Japan | ³Department of Orthodontics and Dentofacial Orthopedics, Osaka University Graduate School of Dentistry, Osaka, Japan | ⁴Bioinformatics Research Unit, Osaka University Graduate School of Dentistry, Osaka, Japan | ⁵Department of Microbiology, Osaka University Graduate School of Dentistry, Osaka, Japan | ⁶Center for Infectious Diseases Education and Research, Osaka University, Osaka, Japan | ⁷Laboratory for Human Immunology (Single Cell Genomics), WPI Immunology Frontier Research Center, Osaka University, Osaka, Japan | ⁸Genome Editing Research and Development Unit, Osaka University Graduate School of Dentistry, Osaka, Japan

Correspondence: Kenji Hata (hata.kenji.dent@osaka-u.ac.jp)

Received: 27 July 2024 | **Revised:** 1 November 2024 | **Accepted:** 6 November 2024

Funding: This work was supported by the Japan Society for the Promotion of Science.

Keywords: growth plate chondrocyte | pre-hypertrophic chondrocyte | Serinc5 | single-cell RNA-seq | Sox9

ABSTRACT

The growth plate is the primary site of longitudinal bone growth with chondrocytes playing a pivotal role in endochondral bone development. Chondrocytes undergo a series of differentiation steps, resulting in the formation of a unique hierarchical columnar structure comprising round, proliferating, pre-hypertrophic, and hypertrophic chondrocytes. Pre-hypertrophic chondrocytes, which exist in the transitional stage between proliferating and hypertrophic stages, are a critical cell population in the growth plate. However, the molecular basis of pre-hypertrophic chondrocytes remains largely undefined. Here, we employed scRNA-seq analysis on fluorescently labeled growth plate chondrocytes for their molecular characterization. Serine incorporator 5 (*Serinc5*) was identified as a marker gene for pre-hypertrophic chondrocytes. Histological analysis revealed that *Serinc5* is specifically expressed in pre-hypertrophic chondrocytes, overlapping with Indian hedgehog (*Ihh*). *Serinc5* represses cell proliferation and *Col2a1* and *Acan* expression by inhibiting the transcriptional activity of Sox9 in primary chondrocytes. Chromatin profiling using ChIP-seq and ATAC-seq revealed an active enhancer of *Serinc5* located in intron 1, with its chromatin status progressively activated during chondrocyte differentiation. Collectively, our findings suggest that *Serinc5* regulates sequential chondrocyte differentiation from proliferation to hypertrophy by inhibiting Sox9 function in pre-hypertrophic chondrocytes, providing novel insights into the mechanisms underlying chondrocyte differentiation in growth plates.

Kenji Hata, Kanta Wakamori, and Akane Hirakawa-Yamamura are contributed equally.

This is an open access article under the terms of the [Creative Commons Attribution-NonCommercial-NoDerivs](https://creativecommons.org/licenses/by-nc-nd/4.0/) License, which permits use and distribution in any medium, provided the original work is properly cited, the use is non-commercial and no modifications or adaptations are made.

© 2024 The Author(s). *Journal of Cellular Physiology* published by Wiley Periodicals LLC.

1 | Introduction

Most bones are generated through endochondral bone development, with growth plate chondrocytes playing a crucial role. Bone growth relies on the continuous proliferation of chondrocytes until the closure of the epiphyseal growth plates. Congenital abnormalities in chondrocyte differentiation and proliferation cause skeletal dysplasia, including achondroplasia caused by *FGFR3* mutation (Ornitz and Legeai-Mallet 2017). Thus, understanding the mechanisms underlying chondrocyte differentiation and function is essential for uncovering the pathophysiology of skeletal dysplasia.

The growth plate contains various chondrocytes originating from undifferentiated mesenchymal cells derived from the mesoderm and neural crest (Olsen, Reginato, and Wang 2000). The condensation of undifferentiated mesenchymal cells triggers chondrocyte lineage commitment, followed by differentiation into proliferating, pre-hypertrophic, and hypertrophic chondrocytes. This differentiation occurs along the direction of bone elongation, forming a characteristic hierarchical columnar structure of chondrocytes—the growth plate (Kronenberg 2003; Long and Ornitz 2013). Histologically, the growth plate mainly comprises round, proliferating, and hypertrophic chondrocytes. These cells exhibit unique shapes and differential gene expression during their differentiation stages, with markers such as *Col2a1* (Lefebvre et al. 1996), *Col11a2* (Tsumaki et al. 1998), and *Aggrecan* (*Acan*) (Lauing et al. 2014) for round and proliferating chondrocytes and *Col10a1* (Knuth et al. 2019) and matrix metalloprotein13 (*Mmp13*) (Inada et al. 2004) for hypertrophic chondrocytes. Transcription factors such as SRY-box transcription factor 9 (*Sox9*) and its transcriptional partners *Sox5* and *Sox6* directly regulate *Col2a1* and *Acan* expression in proliferating chondrocytes, while runt-related transcription factor 2 (*Runx2*) regulates *Col10a1* and *Mmp13* expression in hypertrophic chondrocytes.

Pre-hypertrophic chondrocytes though few, exist in the transition stage from proliferating to hypertrophic chondrocytes, forming a thin cell layer in the growth plate. Pre-hypertrophic chondrocytes stop cell proliferation and increase cell volume. They dramatically change gene expression by inhibiting *Col2a1* and *Acan* expression while promoting *Col10a1*. Indian hedgehog (*Ihh*), predominantly produced by pre-hypertrophic chondrocytes, regulates these processes through parathyroid hormone-related peptide (PTHrP)-dependent and independent mechanisms (Kobayashi et al. 2002; Mak et al. 2008). *Ihh* gene deletion causes severe skeletal defects due to delayed chondrocyte hypertrophy. However, *Ihh* is not sufficient to account for the multiple roles of pre-hypertrophic chondrocytes, and hypertrophic chondrocytes are still detectable in *Ihh*-deficient mice (Amano, Densmore, and Lanske 2015; Razzaque et al. 2005; St-Jacques, Hammerschmidt, and McMahon 1999). These reports suggest that unknown molecules expressed in pre-hypertrophic chondrocytes also regulate chondrocyte differentiation and skeletal development. Conventional methods, such as bulk RNA sequencing, fail to analyze pre-hypertrophic chondrocyte genes due to their limited resolution in distinguishing specific cell populations. However, single-cell RNA sequencing (scRNA-seq) has emerged as a powerful tool for unraveling cellular heterogeneity at the single-cell level. Thus,

scRNA-seq analysis of growth plate chondrocytes allows researchers to not only identify specific genes in pre-hypertrophic chondrocytes but also uncover the mechanisms underlying chondrocyte differentiation.

Serine Incorporator 5 (*Serinc5*) belongs to the *Serinc* family of transmembrane proteins, which facilitate serine incorporation into phosphatidylserine and sphingolipids (Inuzuka, Hayakawa, and Ingi 2005). *Serinc* proteins regulate lipid biosynthesis by directly binding to key enzymes involved in sphingolipid biosynthesis and serine palmitoyltransferase, suggesting that *Serinc5* coordinates serine and serine-derived lipid synthesis (Inuzuka, Hayakawa, and Ingi 2005). Additionally, recent studies show that *Serinc5* inhibits HIV infection at the entry step through the HIV accessory protein Nef (Rosa et al. 2015; Usami, Wu, and Göttinger 2015). *Serinc5* enhances NF- κ B inflammatory signaling through interaction with tumor necrosis factor receptor-associated factor (TRAF6), exerting antiviral effects (Zeng et al. 2021). These findings imply multiple biological functions for *Serinc5* in addition to serine metabolism in various tissues.

In this study, we conducted scRNA-seq analysis of fluorescently labeled growth plate chondrocytes to classify growth plate chondrocytes based on gene expression and identified *Serinc5* as a specific marker gene for pre-hypertrophic chondrocytes. *Serinc5* inhibits cell proliferation and *Sox9*-dependent *Col2a1* and *Acan* expression in primary chondrocytes, and *Serinc5* expression is epigenetically regulated during chondrocyte differentiation. Our findings provide novel insights into the mechanisms underlying chondrocyte differentiation in growth plates.

2 | Materials and Methods

2.1 | Mice

All animal experiments were approved by the Osaka University Institute Animal Experiment Committee and conducted in accordance with regulatory guidelines.

Col11a2-enh-Cre mice were a generous gift from Dr. Noriyuki Tsumaki at Osaka University (Iwai et al. 2008). *Rosa26-CAG-loxP-stop-loxP-ZsGreen* mice (Ai6(RCL-ZsGreen), JAX007906) were obtained from The Jackson Laboratory (Madison et al. 2010). Male *Col11a2-enh-Cre* mice were crossed with female *Rosa26-CAG-loxP-stop-loxP-ZsGreen* mice to produce *Col11a2-ZsGreen* mice. Tail biopsies were performed under anesthesia, and genomic DNA was collected from the tail samples and used for mouse genotyping. Primers used for mouse genotyping are listed in Table S1.

2.2 | Immunohistochemistry

Limbs from E15.0 and newborn *Col11a2-ZsGreen* mice were harvested, fixed in 4% buffered paraformaldehyde, embedded in paraffin, and cut into 6- μ m-thick sections. Paraffin-embedded sections were deparaffinized, rehydrated, and stained with hematoxylin and eosin (H&E). For immunohistochemical

analysis, antigen retrieval was performed using 0.5% hyaluronidase (H3884, Sigma-Aldrich) in phosphate-buffered saline (PBS) at 37°C for 10 min, followed by blocking with 1% bovine serum albumin in PBS. Immunohistochemistry employed anti-collagen type 1 (AB765P, Sigma-Aldrich) and anti-collagen Type 2 (7050, Chondrex) antibodies at 1:200 (v/v). Immunoreactivity was visualized with Alexa Fluor 555 dye-conjugated anti-rabbit IgG (A-21428, Invitrogen) and Alexa Fluor 555 dye-conjugated anti-mouse IgG (A-21422, Invitrogen), and counterstaining was performed with 4',6-diamidino-2-phenylindole per the manufacturer's protocol.

2.3 | scRNA-Seq Analysis

2.3.1 | Single-Cell Preparation

Limbs from *Col11a2-ZsGreen* mice at E15.0 were harvested and cut into small pieces using scissors and blades. Dissected tissues were then incubated with 0.25% Collagenase Type 2 (CLS2, Worthington Biochemical Corporation) in Dulbecco's modified Eagle's medium (DMEM; Sigma-Aldrich, USA) at 37°C for 2 h to dissociate into single cells. Cells were filtered through a 40 µm cell strainer (BD Biosciences) into a 50 ml tube and centrifuged at 300 × g for 5 min to collect cells. The cells were then resuspended in PBS. ZsGreen-positive cells were sorted using fluorescence-activated cell sorting [FACSaria (BD Biosciences)] and resuspended to 1000 cells/µL in PBS with 0.04% BSA following the 10× Genomics cell preparation protocol.

2.3.2 | Library Preparation and Sequencing

Sorted single cells were processed using the 10× Genomics Chromium controller to generate Gel Beads-in-emulsion (GEMs) with the Chromium Next GEM Single Cell 3' Reagent Kits v3.1. Subsequently, the Gel Beads were dissolved, and the cell lysate was incubated with reverse transcription (RT) reagents to produce barcoded cDNA followed by cDNA amplification, which was then amplified and used for 3' gene expression library construction. The cDNA libraries were sequenced using a NovaSeq. 6000 (Illumina, USA).

2.4 | Data Processing of scRNA-Seq Analysis

Sequencing data were first processed using Cell Ranger-7.1.0 and aligned to the mouse genome (mm10). The processed data were subsequently analyzed using Seurat Ver. 4.1.0 (Hao et al. 2021). Cells with fewer than 200 genes, more than 6000 genes, or over 5% mitochondrial read content were filtered out. After removing low-quality cells, we performed data analysis as follows: normalized the data (command: `NormalizeData`), identified highly variable features (command: `FindVariableFeatures`), cell-cycle scoring (command: `CellCycleScoring`) and regression (command: `ScaleData` (vars. to. regress=c("S.Score", "G2M.Score"))), scaled the data (command: `ScaleData`), linear dimensional reduction (command: `RunPCA`), determined data set dimensionality, clustered the cells (command: `FindNeighbors` and `FindClusters`), and ran Uniform Manifold

Approximation and Projection (UMAP) (command: `RunUMAP`). Cluster-specific genes were determined using default settings.

2.5 | In Situ Hybridization

The in situ hybridization protocol was as previously described (Yoshida et al. 2015). Briefly, tissues harvested from E15.0 C57Bl/6 mice were fixed in 4% paraformaldehyde and embedded in paraffin. Tissue blocks were cut into 4-µm-thick sections. Digoxigenin (DIG)-11-UTP-labeled single-stranded RNA probes were prepared using the DIG RNA labeling kit (Roche) following the manufacturer's instructions. We used fragments of mouse *Serinc5* (0.64 kb), *Col10a1* (0.65 kb), and *Ihh* (0.57 kb) cDNA to generate antisense probes. *Col10a1* and *Ihh* cDNA fragments were provided by Dr. Noriyuki Tsumaki (Department of Tissue Biochemistry, Graduate School of Medicine and Frontier Biosciences, Osaka University, Suita, Osaka, Japan). The *Serinc5* cDNA fragment was generated by PCR using specific primer pairs (Fwd: 5'-TGAAAGTCTGGCGCTATGTG-3', Rev: 5'-TCCCTTCTTGACGTTCTGCT-3'). Signals were detected using an alkaline phosphatase-conjugated anti-DIG antibody (11093274910; Roche).

2.6 | Micromass Culture

Micromass cultures of limb bud mesenchymal cells were performed as previously described (Takigawa et al. 2010). The anterior and posterior limb buds of E12.5 wild-type embryos were harvested and digested in DMEM containing 0.1% collagenase type 2. Cells were dissociated by pipetting and centrifuged at 300 × g for 5 min. The pellet was resuspended and cultured in DMEM with 10% fetal bovine serum (FBS) at 37°C in a humidified 5% CO₂ incubator. The culture medium was then changed into α-MEM with 10% FBS, 50 µg/mL ascorbic acid, and 10 mmol/L β-glycerophosphate.

2.7 | Reverse Transcription-Quantitative Polymerase Chain Reaction (RT-QPCR)

Cells were washed with cold PBS, and total RNA was isolated using the NucleoSpin RNA Plus kit. cDNA was synthesized with ReverTra Ace qPCR RT Master Mix (TOYOBO, Osaka, Japan). cDNA was amplified with Eagle Taq Universal Master Mix (ROX) on the StepOnePlus Real-Time PCR System (Applied Biosystems, Foster City, CA, USA). Primers and Taq-Man probes used for cDNA amplification are listed in Table S2. mRNA expression was normalized to β-actin expression levels.

2.8 | Cell Culture and Reagents

The mouse fibroblast-like cell line C3H10T1/2 (RCB0247) and the mouse teratocarcinoma cell line ATDC5 (RCB0565) were provided by RIKEN BRC through the National BioResource Project of MEXT/AMED, Japan. The cells were cultured at 37°C in a humidified 5% CO₂ incubator in DMEM containing 10%

FBS or a 1:1 mixture of DMEM and Ham's F-12 medium (Sigma-Aldrich) with 10% FBS. An insulin-transferrin-sodium selenite supplement (ITS; Roche, Basel, Switzerland) was used to induce chondrocyte differentiation in ATDC5 cells.

Primary chondrocytes were isolated following a protocol described by Gartland et al. (Gartland et al. 2005). Briefly, rib cartilage from newborn mice was dissected and digested with 2.5 mg/mL Collagenase Type 2 (Worthington) for 1 h at 37°C to remove soft tissues. After washing with PBS, ribs were incubated with 2.5 mg/mL Collagenase Type 2 for an extra 6 h at 37°C to isolate chondrocytes. Primary chondrocytes were collected by centrifugation and resuspended in DMEM with 10% FBS and antibiotics. Cells within two passages were used as primary chondrocytes. C57BL/6 mouse bone marrow MSCs were obtained from Cyagen (#MUBMX-01001; USA) and cultured in DMEM with 10% FBS at 37°C in a humidified 5% CO₂ incubator.

2.9 | Generation of Lentivirus

Serinc5 cDNA was subcloned into the pLVSI-CMV Puro vector (TAKARA Bio, Japan) and transfected with lentiviral high-titer packaging mix (TAKARA) into Lenti-X 293 T cells (TAKARA). After 72 h of transfection, supernatants containing lentiviral particles were collected and concentrated using a Lenti-X Concentrator (Clontech Laboratories) according to the manufacturer's protocol. Primary chondrocytes were infected with lentiviral particles using polybrene (7 µg/mL). The medium was replaced 24 h after infection, and cells were cultured with 1 µg/mL puromycin to select puromycin-resistant clones. An empty pLVSI-CMV Puro vector was used as a control.

2.10 | Generation of Adenovirus

Adenoviral cDNAs of flag-tagged mouse Sox9 were amplified by PCR and subcloned into pAXCAwt vectors (TAKARA Bio, Japan). Recombinant adenoviruses were generated using the COS-TPC method by transfecting a recombinant cosmid and the DNA-TPC adenovirus genome into 293 cells (Hata et al. 2013). Primary limb bud cells were infected with adenoviruses at a multiplicity of infection of 20 unless otherwise indicated.

2.11 | Cell Proliferation Assay

The cell proliferation assay was performed using the Premix WST-1 Cell Proliferation Assay System (Roche), according to the manufacturer's instructions. Briefly, primary chondrocytes were cultured in 24-well plates (10,000 cells/well) and incubated at 37°C in a 5% CO₂ atmosphere. On Days 1 and 2, the cell proliferation reagent was added to each well and incubated for 1 h. Absorbance was measured using a Model 550 microplate reader.

2.12 | Western Blot Analysis

Cells were rinsed twice with PBS and solubilized in lysis buffer [20 mM HEPES (pH 7.4), 150 mM NaCl, 1 mM EGTA, 1.5 mM

MgCl₂, 10% glycerol, 1% Triton X-100, 10 µg/mL aprotinin, 10 µg/mL leupeptin, 1 mM 4-(2-aminoethyl) benzene sulfonyl fluoride hydrochloride, and 0.2 mM sodium orthovanadate]. Lysates were centrifuged at 15,000 × g for 10 min at 4°C. The supernatant was boiled in sodium dodecyl sulfate (SDS) sample buffer containing 0.5 M β-mercaptoethanol for 5 min. Samples for Serinc5 diluted with SDS sample buffer were prepared without boiling. Proteins were separated by SDS-polyacrylamide gel electrophoresis, transferred to a nitrocellulose membrane, immunoblotted with a primary antibody, and visualized with horseradish peroxidase-coupled anti-mouse or anti-rabbit IgG using an enhanced chemiluminescence detection kit (Immunostar LD; WAKO, Osaka, Japan). Primary antibodies against Serinc5 (ab204400; Abcam), Sox9 (AB5535; Sigma-Aldrich), and β-actin (M177-3; MBL) were used.

2.13 | Reporter Assay

The *Col2a1* gene promoter (−89 to +16) and four 48-base pair tandem repeats of the Sox9 binding element present in the first intron of the *Col2a1* gene were introduced upstream of the luciferase gene (Muramatsu et al. 2007). The aggrecan promoter (−100 to +110) and two copies of the A1 enhancer element located −9477 bp upstream were ligated into pGL4 basic plasmids according to previous reports (Han and Lefebvre 2008). Reporter genes were cotransfected with Sox9 or Serinc5 expression vectors and Renilla luciferase into cells using the X-treme Gene9 DNA Transfection Reagent (Sigma-Aldrich). After 48 h of transfection, cells were lysed, and luciferase activity was measured using specific substrates in a luminometer (Promega) following the manufacturer's protocol. Luciferase activity was normalized to Renilla's activity.

2.14 | Assay for Transposase-Accessible Chromatin (ATAC)-Seq

Fragmentation and amplification of ATAC-seq libraries were constructed following Buenrostro et al. (Buenrostro et al. 2015). Briefly, MSCs were collected and resuspended in cold PBS. Approximately 50,000 cells were lysed using lysis buffer (10 mM Tris-HCl, pH 7.4, 10 mM NaCl, 3 mM MgCl₂, and 0.1% IGEPAL CA-630), and a transposition reaction was performed with the Tn5 Transposase (Illumina Catalog #FC121-1030) at 37°C for 30 min. DNA samples were amplified and purified with NucleoSpin Gel and PCR Clean-up (Marcheray Nagel). Paired-end sequencing (100 bp) was conducted on an Illumina HiSeq sequencer (Illumina, USA).

2.15 | Data Analysis of ATAC-Seq and ChIP-Seq

ATAC-seq and ChIP-seq, datasets of primary chondrocytes (GSE237889), were obtained from the GEO database (Ichiyama-Kobayashi et al. 2024). ATAC-seq and ChIP-seq reads were mapped to the mm10 reference sequence using Bowtie2 (ver. 2.4.4) (Langmead and Salzberg 2012), and duplicate reads were removed with Picard (Ver 2.26.9, <https://broadinstitute.github.io/picard/>). ATAC-seq and ChIP-seq peaks were detected using

MACS2 (ver.2.2.4) (J. Feng et al. 2012) with default settings (q-value, 0.05) and visualized with IGV (ver.2.13.0).

2.16 | ChIP QPCR

ATDC5 cells treated with or without ITS were cross-linked with 1% methanol-free formaldehyde for 5 min. Cross-linking was quenched with 1 M glycine for 5 min, and the cells were washed three times with cold PBS. Cells were lysed with lysis buffer, and cross-linked chromatin was sonicated with a Covaris M220. Sonicated chromatin was immunoprecipitated using an anti-H3K27ac antibody (D5E4; Cell Signaling Technology) at 4°C overnight. ChIP samples were washed, eluted with elution buffer at 65°C for 30 min, and reverse cross-linked at 65°C overnight. DNA was purified using a DNA purification buffer and spin columns (Cell Signaling Technology). Quantitative analysis of ChIP assays was performed by real-time PCR using specific primer pairs for the *Serinc5* enhancer (Fwd: 5'-ACTTCTACCTGTATGTGGATCA-3', Rev: 5'-GCTGCTGAAGTGGCCTAATT-3').

2.17 | Alcian Blue Staining

Cells were washed with PBS and fixed with 3.7% formaldehyde in PBS for 10 min at room temperature. Subsequently, the cells were stained with 1% Alcian Blue in 5% acetic acid for 10 min.

2.18 | Statistical Analysis

Data were statistically analyzed using the unpaired Student's *t*-test for comparisons between the two groups. For more than two groups, we used one-way or two-way analysis of variance (ANOVA) followed by Tukey's multiple comparison test. Unless otherwise stated, we performed two or three independent in vitro experiments, including RT-qPCR and western blot. A *p*-value of < 0.05 was considered statistically significant.

3 | Results

3.1 | Generation and Characterization of *Col11a2-ZsGreen* Mice

To conduct scRNA-seq analysis of growth plate chondrocytes, we used *Col11a2-enh-Cre* mice which exhibit more restricted Cre recombinase activity in chondrocytes than *Prx1-Cre* and *Col2a1-Cre* (Couasnay et al. 2021; Iwai et al. 2008). We crossed *Col11a2-enh-Cre* mice with *ROSA26-CAG-LSL-ZsGreen* mice, generating *Col11a2-ZsGreen* mice (Figure 1a). Hind limbs at E15.0 and P0 were harvested to examine ZsGreen expression patterns and compared with those of Col1 and Col2 using immunohistochemical analysis. In P0 mice, many ZsGreen-positive cells were Col1 positive in bone marrow, indicating ZsGreen labeling in osteoblasts (Figure S1a,b). In contrast, primary ossification centers were not formed at E15.0 limbs, and most ZsGreen-positive cells were Col2-positive (Figure 1b). Immunohistochemical analysis revealed that Col1-positive perichondral cells adjacent to the hypertrophic chondrocytes

were labeled with ZsGreen (Figure 1c). Because these cells give rise to osteoblasts and form a bone collar (Hojo et al. 2012), ZsGreen-labeled cells include a small number of pre-osteoblasts and osteoblasts. ZsGreen expression was also detected in interzone cells which are critical for articular cartilage development, (Figure 1d) (Pacifici et al. 2006).

Characterizing hypertrophic chondrocytes in E15.0 *Col11a2-ZsGreen* mice, we found that approximately one-third of femur growth plates were hypertrophic chondrocytes (Figure 1e). Interestingly, ZsGreen-labeled hypertrophic chondrocytes were positive for Col10, a marker gene for pre and early hypertrophic chondrocytes, but negative for *Mmp13*, which is expressed in terminal hypertrophic chondrocytes (Figure 1e) (Yang et al. 2014). These findings collectively suggest that E15.0 *Col11a2-ZsGreen* mice are suitable for analyzing pre-hypertrophic chondrocytes using scRNA-seq.

3.2 | ScRNA-Seq Analysis of Mouse Growth Plate Chondrocytes

We isolated 6797 ZsGreen-labeled cells from E15.0 *Col11a2-ZsGreen* mice limbs using FACS (Figure 2a). These cells underwent scRNA-seq analysis with the 10X Genomics Chromium Single Cell Gene Expression System and subsequent computational analysis using Seurat v4 (Figure 2a) (Hao et al. 2021). Initial profiling of ZsGreen-labeled cells using UMAP identified 18 clusters (Figure S2a). Although we observed *Col2a1* expression in non-mesenchymal lineage cells, including macrophages, mast cells, epithelial cells, and endothelial cells, *Col2a1* expression in these was remarkably lower compared to that in mesenchymal cells (Figures S2a,b).

We then re-clustered the subset of mesenchymal cell clusters using UMAP and identified eight clusters (Figure 2b). Approximately 70% of cells were in three clusters (clusters 1, 2, and 3), characterized by round chondrocytes with high *Sox9*, *Col2a1*, and *Acan* expression (Figure 2b-f). The expression of *Gdf5* and *Pthlh*, known as PTHrP, was enriched in cluster 0 (Figure 2b,e,f), suggesting that cluster 0 includes cells at most epiphyseal ends of the growth plate, which contribute to articular cartilage (Koyama et al. 2008). Cluster 4 included proliferating chondrocytes with high Topoisomerase IIA (Top 2a) expression (Figure 2b,e). Consistent with Col1 immunohistochemistry results (Figure 1d,e), differential gene expression analysis revealed *Col1a1* (high) and *Col2a1* (low) clusters (clusters 6 and 7) (Figure 2b,d,e,f). Cluster 7 expressed osteoblastic genes, including *Alpl* and *Ibsp*, with abundant *Col1a1* expression, while cluster 6 did not. These data indicate that cluster 6 contains interzone cells and cluster 7 contains osteoblasts. Cluster 5, representing 5% of total cells, showed specific *Ihh* and *Col10a1* expression, markers of pre-hypertrophic chondrocytes (Figure 2b,e). Feature plot analysis highlighted a distinct cluster of *Ihh*-positive cells (Figure 2f, arrowhead). These results suggest the successful identification of a pre-hypertrophic chondrocyte cluster.

3.3 | Identification of *Serinc5* as a Specific Marker Gene for Pre-Hypertrophic Chondrocytes

To identify potential marker genes for pre-hypertrophic chondrocytes, we analyzed differentially expressed genes (DEGs) in

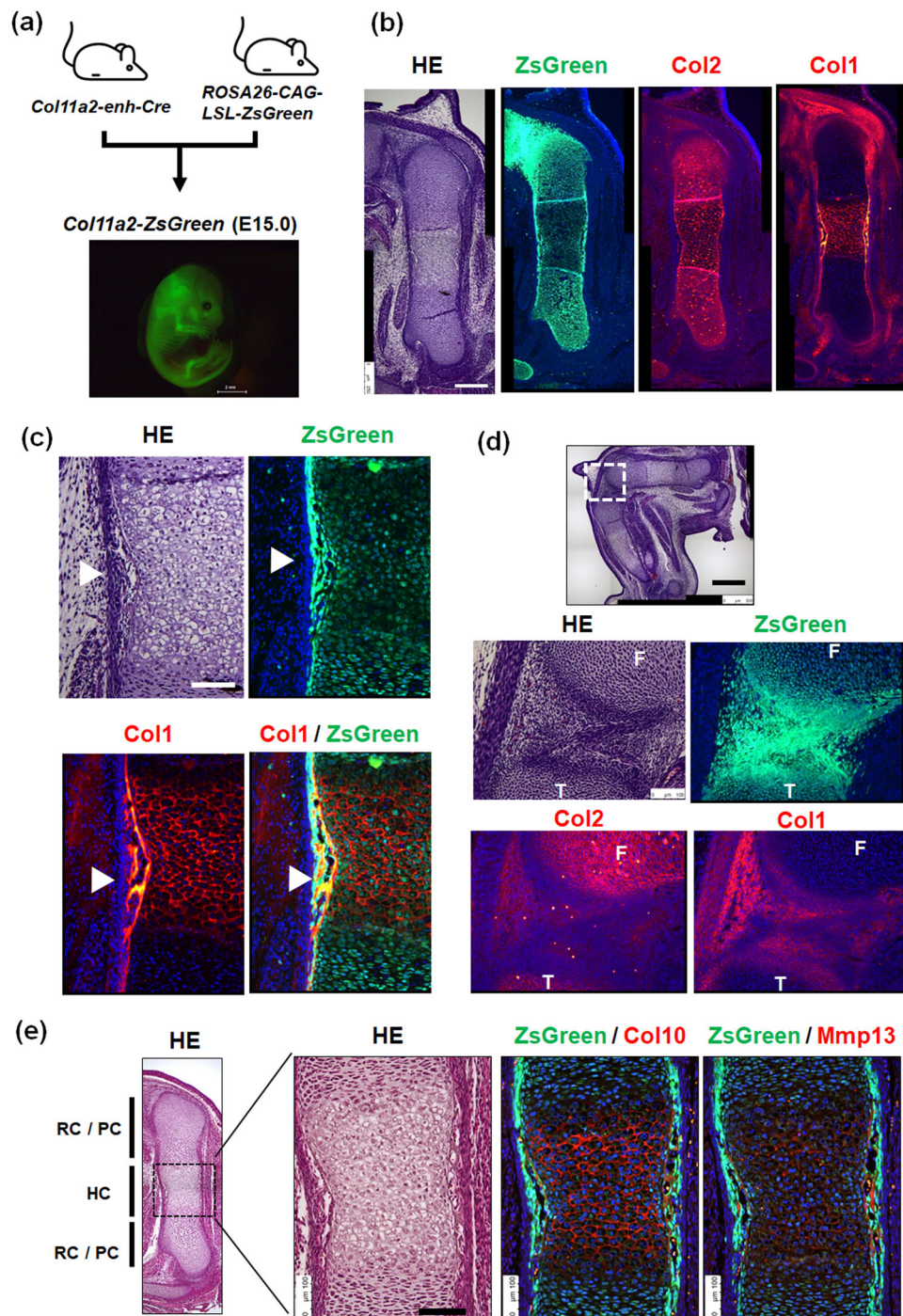


FIGURE 1 | Generation and immunohistochemical analysis of E15.0 *Col11a2-ZsGreen* mice. (a) Schematic model to generate *Col11a2-ZsGreen* mice. E15.0 embryo photographed using fluorescence microscopy. Scale bar: 1 mm. (b) Immunostaining for Col2 and Col1 in femur from E15.0 *Col11a2-ZsGreen* mice. Scale bar: 250 μ m. (c) Immunostaining for Col1 in perichondrium from E15.0 *Col11a2-ZsGreen* mice femur. Arrowheads indicate Col1-positive osteoblasts overlapping with ZsGreen. Scale bar: 100 μ m. (d) Immunostaining for Col2 and Col1 in interzone from E15.0 *Col11a2-ZsGreen* mice femur. Higher magnification images of the boxed area (upper panel) are shown in the lower panel. Scale bar: 100 μ m. F: Femur T: Tibia. (e) Immunostaining for Col10 and Mmp13 in hypertrophic chondrocytes from E15.0 *Col11a2-ZsGreen* mice femur. Scale bar: 100 μ m. HC, hypertrophic chondrocytes; PC, proliferating chondrocytes; RC, round chondrocytes.

each cell cluster (Table S3). Among the top 10 genes identified as cluster 5-specific DEGs were *Col10a1*, *Ihh*, and *Pth1r*, established markers for pre-hypertrophic chondrocytes (Figure 3a). Additionally, *Panx3*, the target of Runx2 expressed in pre-hypertrophic chondrocytes (Iwamoto et al. 2010), was enriched in cluster 5. These findings suggest that the DEGs in

cluster 5 are reliable candidates as marker genes for pre-hypertrophic chondrocytes.

Among the top 10 genes in cluster 5, we focused on *Serinc5* because its expression levels and pattern were comparable to those of *Ihh* and *Panx3* (Figure 3b). In situ hybridization revealed

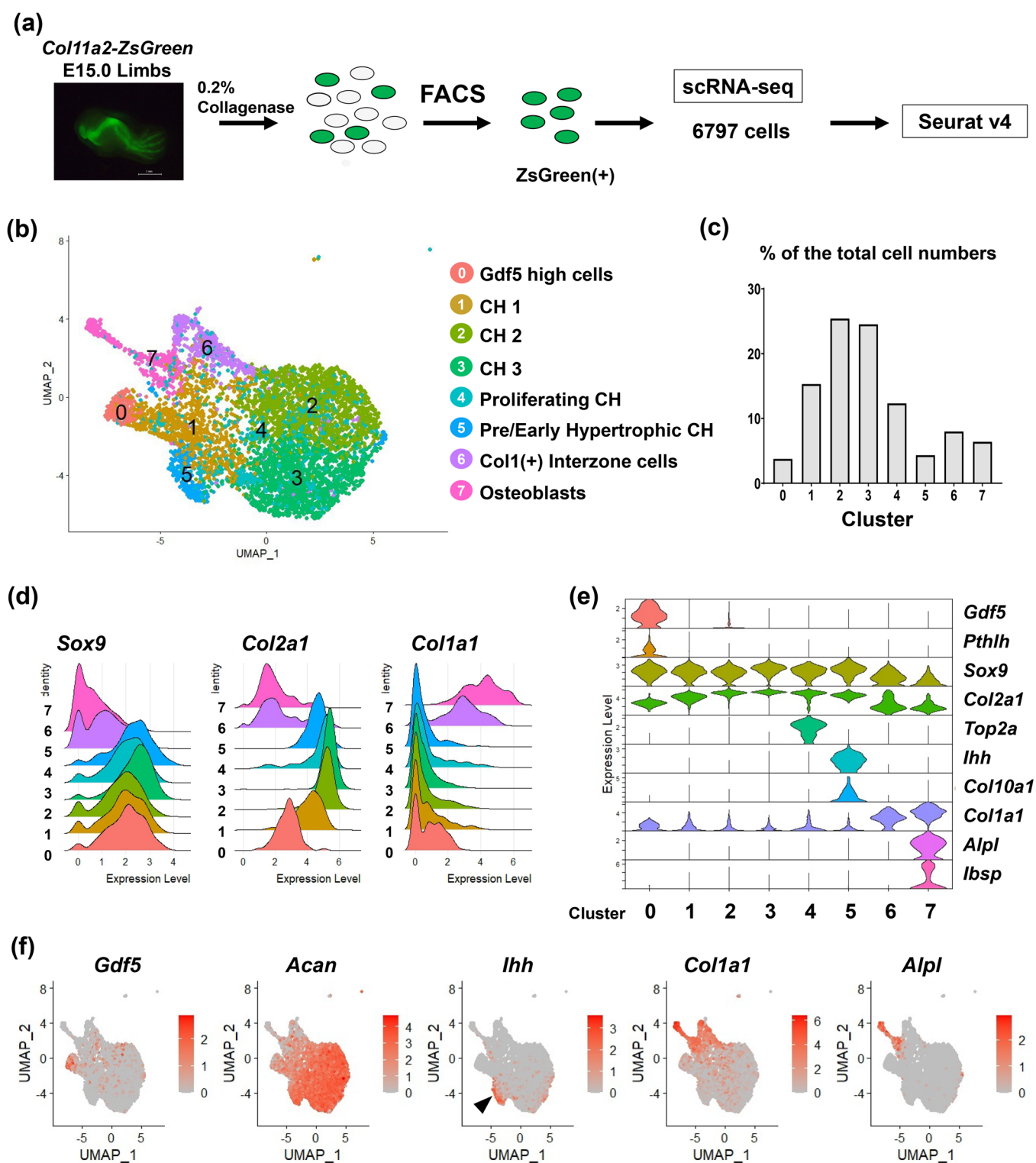


FIGURE 2 | Single-cell RNA-seq analysis of *Col11a2-enh-Cre* marked mesenchymal cells. (a) Strategy for single-cell RNA-seq analysis of growth plate chondrocytes isolated from the limbs of E15.0 *Col11a2-ZsGreen* mice. (b) UMAP plots of ZsGreen-positive cells isolated from the limbs of E15.0 *Col11a2-ZsGreen* mice. CH, chondrocyte. (c) Percentage of total cell numbers in each cluster. (d) Ridgeline plot showing *Sox9*, *Col2a1*, and *Col1a1* expression. (e) Violin plot showing marker gene expression in chondrocytes and osteoblasts. (f) Expression patterns of chondrocyte and osteoblast marker genes in UMAP plots. Arrowheads indicate cluster 5. UMAP, uniform manifold approximation and projection.

specific expression of *Serinc5* in pre-hypertrophic chondrocytes of E15.0 tibial growth plate (Figure 3c), P0 femoral growth plates (Figure S3a,b), and rib cartilages (Figure S4). In contrast, other candidate genes including *Uts2b* (Urotensin 2B), *Cpa6*

(Carboxypeptidase 6), *Cd200*, *Kcnt2* (Potassium channel, sub-family T, member2) were not detected in tibial growth plates (Figure S5a,b). Feature plot analysis demonstrated that *Serinc5* was enriched in cluster 5 and overlapped with *Ihh* (Figure 3d).

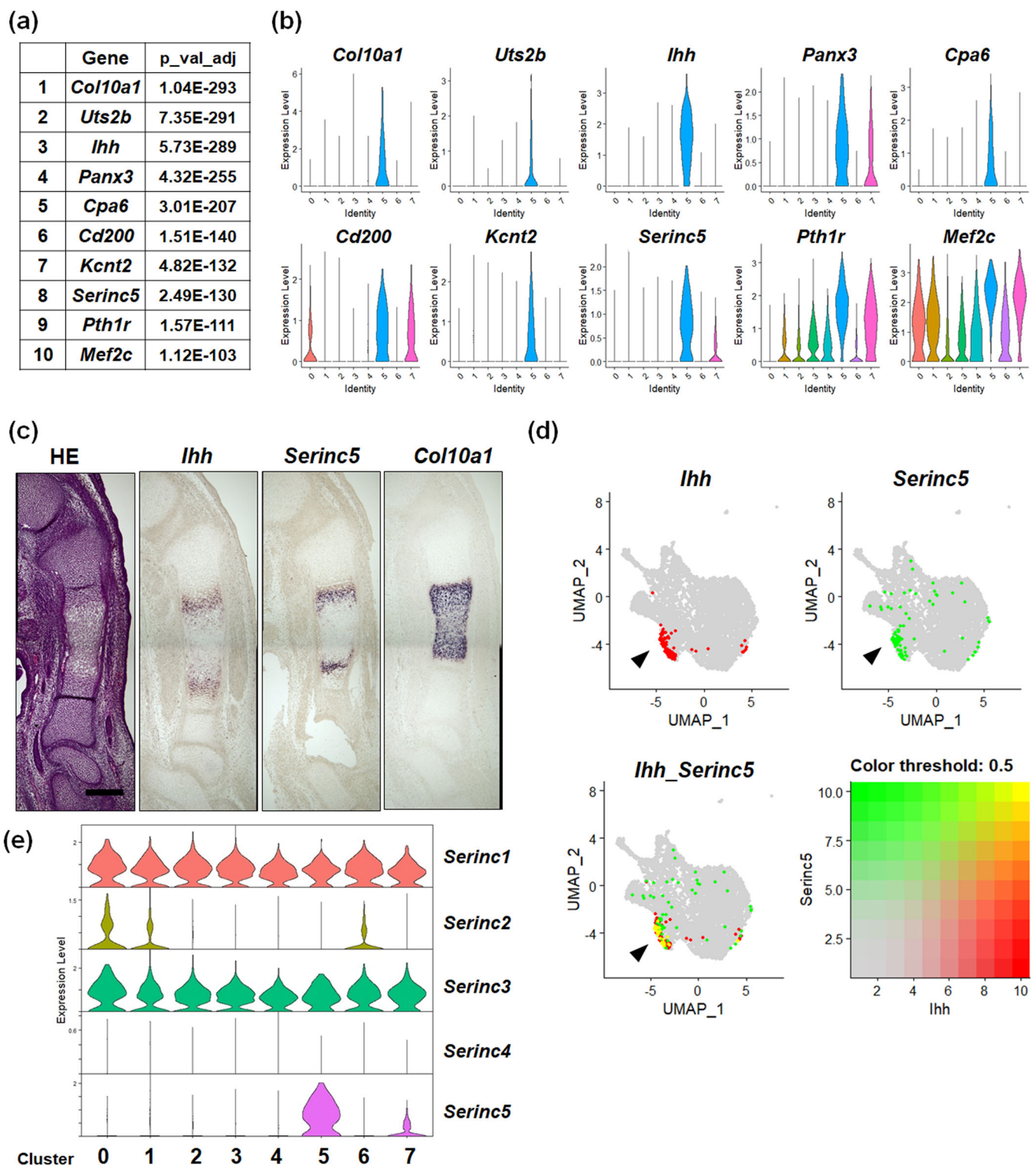


FIGURE 3 | Identification of *Serinc5* as the specific marker gene for pre-hypertrophic chondrocytes. (a) List of 10 significant differentially expressed genes (DEGs) in cluster 5. (b) Violin plot showing the top 10 DEGs in cluster 5. (c) Haematoxylin and eosin (HE) staining and in situ hybridization analysis of *Ihh*, *Serinc5*, and *Col10a1* in growth plate chondrocytes from E15.0 mice tibia. Scale bar: 200 μ m (d) Feature plot illustrating the expression of *Serinc5* and *Ihh*. Arrowheads indicate cluster 5. (e) Violin plot showing the expression of *Serinc* family genes.

scRNA-seq data also indicated ubiquitous expression of *Serinc1* and *Serinc3* in growth plate chondrocytes (Figure 3e).

We then examined the expression pattern of *Serinc5* during chondrocyte differentiation in a micro mass culture

model of limb-bud mesenchymal cells, which mimics the chondrocyte differentiation program from mesenchymal condensation to chondrocyte hypertrophy (Underhill, Dranse, and Hoffman 2014). Marker genes of early chondrogenesis, including *Col2a1*, *Acan*, and *Sox9*, gradually

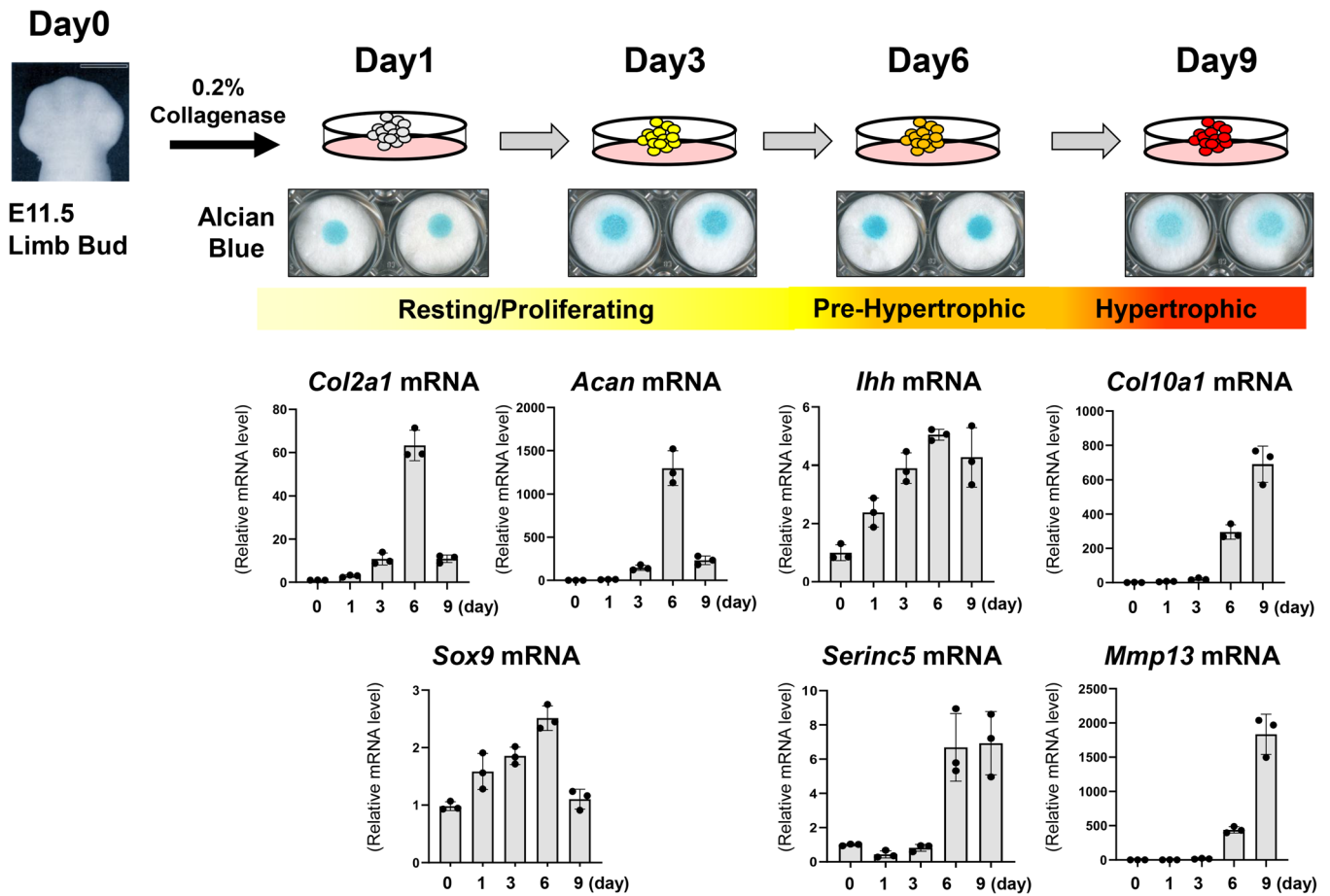


FIGURE 4 | Expression pattern of *Serinc5* during chondrocyte differentiation. The flowchart upper in the panel illustrates the process of micromass culture of mouse limb bud cells. The graphs indicate gene expression of chondrocyte markers and *Serinc5*, determined using RT-qPCR. Data are shown as fold activation normalized to day 0 (means \pm SD, $n = 3$).

increased and reached a maximum on day 6 (Figure 4) and decreased by day 9 when the expression of *Col10a1* and *Mmp13* reached a maximum (Figure 4). The level of Alcian Blue staining was also reduced on day 9 (Figure 4). Notably, the expression of *Ihh* and *Serinc5* reached a maximum on day 6 and remained high during chondrocyte hypertrophy (Figure 4). Taken together, these findings suggest that *Serinc5* is a specific marker gene for pre-hypertrophic chondrocytes.

3.4 | *Serinc5* Inhibits Sox9-Dependent Chondrocyte Gene Expression

We examined whether *Serinc5* regulates chondrocyte differentiation. Pre-hypertrophic chondrocytes stop proliferating and alter chondrocyte gene expression during hypertrophy. Consistent with this, *Serinc5* overexpression in primary chondrocytes significantly decreased cell proliferation (Figure 5a). Although *Serinc5* alone did not affect chondrocyte gene expression, it decreased *Col2a1*, *Acan*, and *Sox9* expression induced by *Bmp2* (Figure 5b). In contrast, the expression levels of pre-hypertrophic and hypertrophic genes, including *Ihh*, *Col10a1*, *Runx2*, and *Sp7*, were not altered (Figure 5c).

We then explored if *Serinc5* inhibits *Col2a1* and *Acan* expression by regulating *Sox9* function. We confirmed that *Serinc5* overexpression did not alter *Sox9* protein levels in primary chondrocytes (Figure 6a). Notably, *Serinc5* decreased *Sox9*-dependent *Col2a1* and *Acan* expression (Figure 6b). A reporter assay with *Col2a1* and *Acan* promoters containing *Sox9* binding elements further demonstrated that *Serinc5* inhibited the transcriptional activity of *Sox9* (Figure 6c). These findings suggest that *Serinc5*, expressed in pre-hypertrophic chondrocytes, negatively regulates chondrocyte differentiation by inhibiting *Sox9* function.

We next examined the molecular mechanism by which *Serinc5* inhibits *Sox9* function. Because *Serinc5* enhances type I interferon (IFN) expression by activating NF- κ B signaling (Zeng et al. 2021) and NF- κ B signaling inhibits *Sox9* transcriptional activity (Murakami, Lefebvre, and de Crombrughe 2000), we explored the effect of NF- κ B inhibitor BAY 11-7082, a selective and irreversible inhibitor of I κ B α phosphorylation, on the inhibitory effect of *Serinc5* on *Sox9* function. *Serinc5* decreased *Sox9*-dependent *Col2a1* and *Acan* expression (Figure S6a) and *Sox9* transcriptional activity (Figure S6b), as expected. However, treatment with BAY 11-7082 further reduced *Col2a1* and *Acan* expression (Figure S6a) but had no effect on *Sox9* transcriptional activity (Figure S6b).

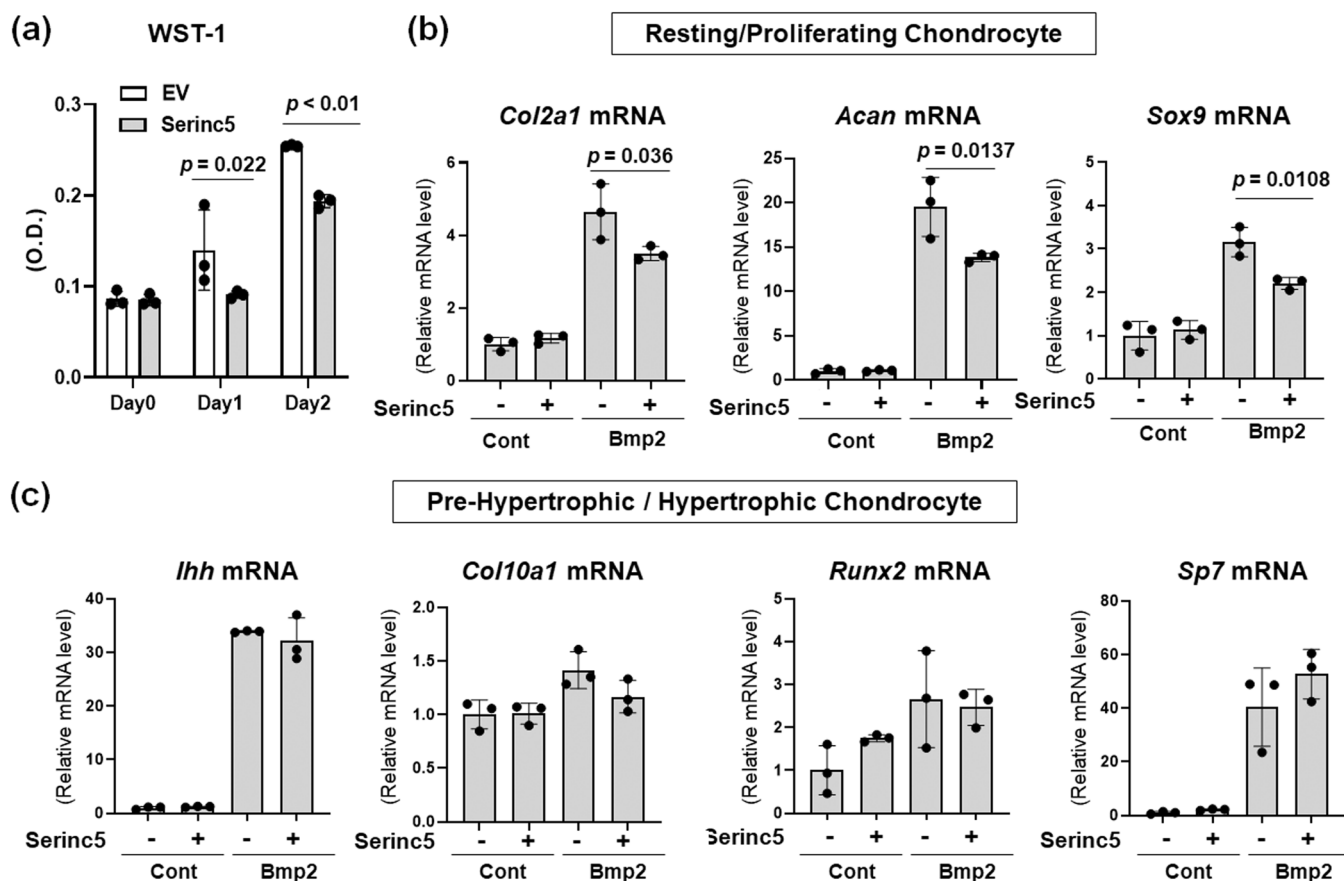


FIGURE 5 | Inhibition of chondrocyte proliferation and differentiation by Serinc5. (a) Proliferation of primary chondrocytes infected with Empty Vector (EV) or *Serinc5* lentivirus cultured for 2 days in a 96-well plate, measured using the WST-1 Proliferation Assay Kit ($n = 3$, Student's t -test). (b, c) Total RNA in primary chondrocytes infected with EV or *Serinc5* lentivirus cultured with or without recombinant BMP2 analyzed by RT-qPCR for marker genes of resting/proliferating chondrocytes (b) and pre-hypertrophic/hypertrophic chondrocytes (c). Data are shown as the mean \pm SD. ($n = 3$, biologically independent samples). Statistical analysis was performed using one-way ANOVA followed by Tukey's multiple comparison test.

3.5 | Epigenetic Regulation of *Serinc5* Expression in Chondrocytes

Finally, we investigated the molecular mechanisms underlying *Serinc5* expression during chondrocyte differentiation. We searched for enhancers associated with *Serinc5* expression using ATAC-seq. Profiling of ATAC-seq peaks in and around *Serinc5* using MSCs and primary chondrocytes identified several chondrocyte-specific open chromatin regions within *Serinc5* (Figure 7a). A 600 bp genomic region (chr13:93,406,733-93,407,307) overlapped with ChIP-seq peaks of H3K27ac, an active enhancer histone mark (Figure 7a, highlighted in gray). The reporter assay further demonstrated the strong enhancer activity of the 300 bp region in primary chondrocytes (Figure 7b).

We then tested if the enhancer activity of this genomic region is activated during chondrocyte differentiation in ATDC5 cells treated with ITS. ITS treatment promoted *Serinc5* expression, as evidenced by RT-qPCR (Figure 7c). ChIP-qPCR using an anti-H3K27ac antibody revealed concomitant enrichment of H3K27ac in the *Serinc5* enhancer in intron 1 (Figure 7d). These data suggest that enhancer activity in intron 1 is associated with *Serinc5* expression in chondrocytes.

4 | Discussion

4.1 | Identification of Pre-Hypertrophic Specific Genes

Growth plate chondrocytes, responsible for skeletal development, are biologically unique cells comprising diverse chondrocytes with various histological features. Understanding the molecular basis underlying the cellular diversity of growth plate chondrocytes is crucial for elucidating skeletal development mechanisms. Conventional experimental approaches analyzing growth plates as bulk tissues have made it challenging to unravel the diversity and hierarchy of these chondrocytes. Here, we identified *Serinc5* as a specific marker gene for pre-hypertrophic chondrocytes. We also found that *Serinc5* regulates chondrocyte differentiation by suppressing *Sox9* function. These findings are expected to advance our understanding of the molecular mechanisms underlying endochondral bone development and the pathophysiology of inherited skeletal disorders.

scRNA-seq analysis is a powerful technique for uncovering cellular heterogeneity in various tissues (Stuart and Satija 2019). Several studies have applied scRNA-seq to growth plate chondrocytes. Haseeb et al. used the distal femur and tibial

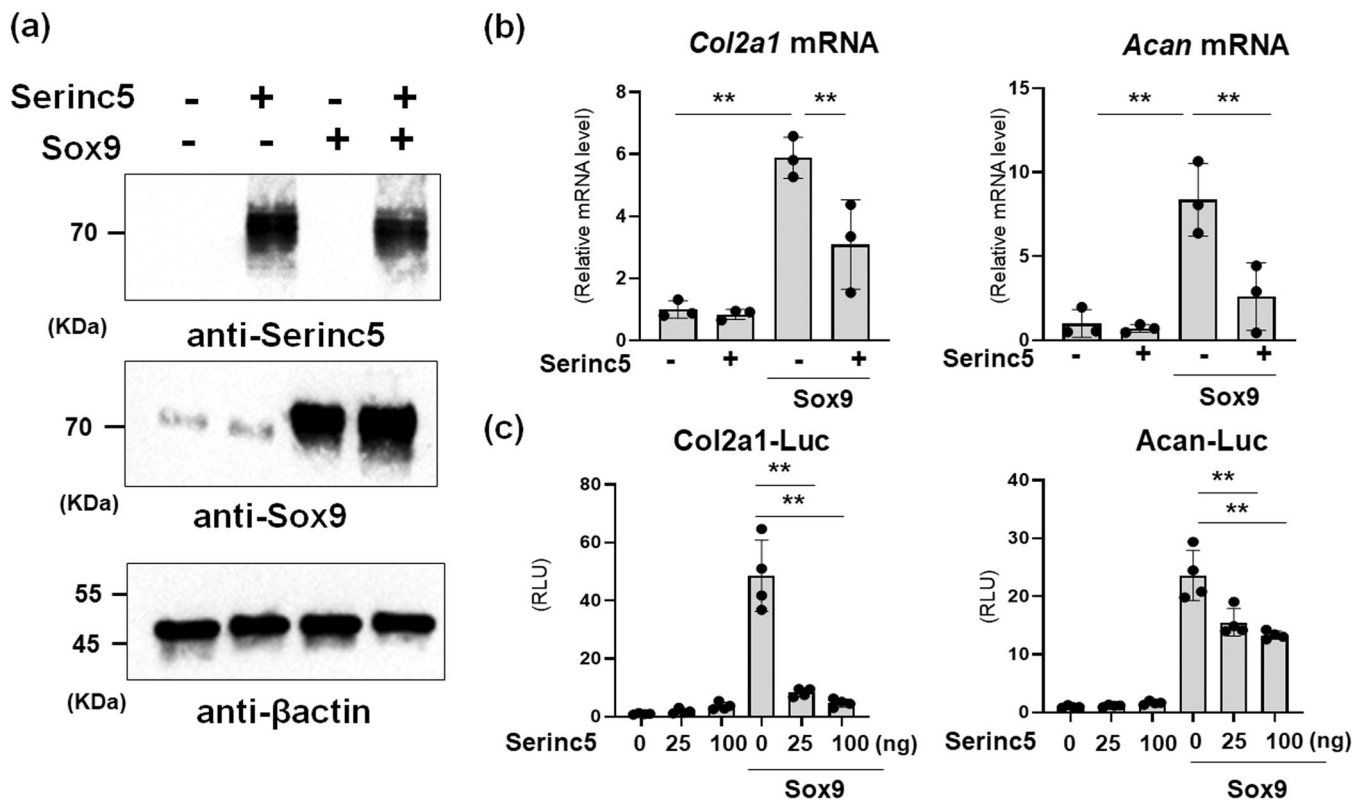


FIGURE 6 | Inhibition of Sox9-dependent chondrocyte gene expression by Serinc5. (a) Immunoblot analysis illustrating the expression levels of Serinc5, Sox9, and β -actin in primary chondrocytes infected with Empty Vector (EV) or Serinc5 lentivirus, followed by Sox9 overexpression. (b) RT-qPCR results showing the relative mRNA levels of *Col2a1* and *Acan* in primary chondrocytes infected with EV or Serinc5 lentivirus followed by Sox9 overexpression. Data are shown as the mean \pm SD. ($n = 3$, biologically independent samples). $**p < 0.01$, one-way ANOVA followed by Tukey's multiple comparison test. (c) Luciferase assay results demonstrating the transcriptional activity of *Col2a1* and *Acan* in C3H10T1/2 cells transfected with *Col2a1* or *Acan* luciferase construct along with EV, Serinc5, or Sox9 expression vectors. Data are shown as the mean \pm SD. ($n = 4$, biologically independent samples). $**p < 0.01$, one-way ANOVA followed by Tukey's multiple comparison test.

epiphyses of postnatal mice to isolate chondrocytes, but contamination with nonskeletal cells, including blood cells, resulted in low accuracy of their scRNA-seq analysis (Haseeb et al. 2021). Flow cytometry-based methods have also been used to isolate chondrocytes from reporter mice, including postnatal *Col2a1-CreER;R26R^{tdTomato}* mice (Mizuhashi et al. 2019) and *Col10a1-CreER;R26R^{tdTomato}* mouse (Long et al. 2022). However, previous scRNA-seq studies have failed to categorize pre-hypertrophic chondrocytes as a distinct cluster and distinguish pre-hypertrophic chondrocytes from mature hypertrophic chondrocytes, likely due to the small ratio of pre-hypertrophic chondrocytes.

To address this, we used E15.0 mice, in which the primary ossification center had not formed, and *Col11a2-enh-Cre* mice, which show more restricted activity in growth plate chondrocytes than *Col2a1-cre* lines (Couasnay et al. 2021). This strategy increased the proportion of pre-hypertrophic chondrocytes, enabling effective investigation of their gene expression patterns. Supporting this notion, highly selective expression of *Ihh*, *Panx3*, and *Pth1r* in cluster 5 was observed in our scRNA-seq data (Figure 3a,b). Additionally, we identified several genes, including *Uts2b*, *Cpa6*, *Kcnt2*, and *Serinc5*, enriched in cluster 5. Most of these have unknown roles in chondrocyte differentiation and skeletal development. It would be interesting to further investigate the roles of cluster 5 genes in chondrocyte differentiation.

In addition to pre-hypertrophic chondrocytes, the characterization of hypertrophic chondrocytes by scRNA-seq analysis is important to understand the molecular basis of skeletal development. However, due to their fragility and large cell volumes, the capture efficiency of hypertrophic chondrocytes is very low. The maximum cell size of single-cell capture by the 10 \times Genomics system is 30 μ m, while the average cell size of hypertrophic chondrocytes is approximately 40 μ m (Cooper et al. 2013). We speculate that this technical limitation led to the failure of our scRNA-seq analysis to detect hypertrophic chondrocytes. Although mRNA is thought to predominantly reside in the cytoplasm, nuclei isolation followed by single nuclear RNA sequencing (snRNAseq) is the best option for identifying marker genes of hypertrophic chondrocytes.

4.2 | Role of Serinc5 in Chondrocyte Differentiation

Serinc5 inhibits cellular proliferation and Sox9-dependent *Col2a1* and *Acan* expression in chondrocytes (Figures 5 and 6). These findings suggest that pre-hypertrophic chondrocytes halt cell proliferation and the transcription of *Col2a1* and *Acan*, supporting chondrocyte hypertrophy. However, the precise molecular mechanism through which Serinc5 inhibits Sox9-dependent *Col2a1* and *Acan* expression remains unclear.

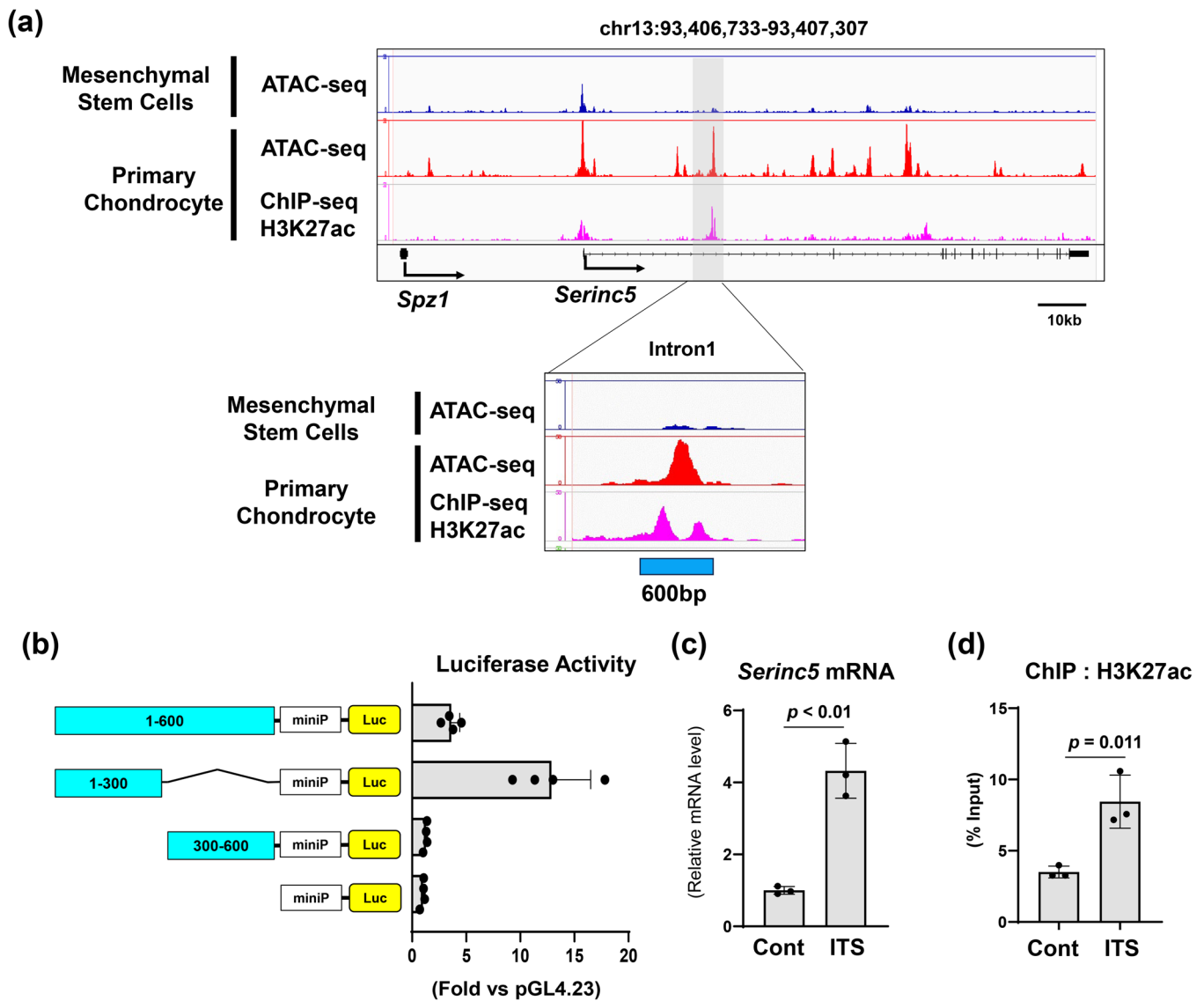


FIGURE 7 | Epigenetic regulation of *Serinc5* in chondrocytes. (a) ATAC-seq and ChIP-seq profiles of the genomic region around mouse *Serinc5* gene in mesenchymal stem cells and primary chondrocytes. Light gray shading magnified in the lower panel highlights the candidate genomic region of the *Serinc5* enhancer in chondrocytes. (b) Luciferase reporter constructs of deletions of *Serinc5* enhancer were transfected into primary chondrocytes. Luciferase activities were measured at 48 h after transfection. Data are shown as the mean \pm SD. ($n = 4$, biologically independent samples). (c) Total RNA isolated from ATDC5 treated with or without ITS was analyzed by RT-qPCR for *Serinc5* gene expression. Data are shown as the mean \pm SD. ($n = 3$, biologically independent samples). Unpaired Student's *t*-test. (d) ChIP-qPCR analysis of *Serinc5* enhancer in ATDC5 cells treated with or without ITS. Sonicated chromatin isolated from ATDC5 cells was immunoprecipitated with an anti-H3K27ac antibody and quantified using specific primers for *Serinc5* enhancer. Data are shown as the mean \pm SD. ($n = 3$, biologically independent samples). Unpaired Student's *t*-test. ITS, insulin, transferrin, selenium.

One predicted mechanism involves nuclear factor κ B (NF- κ B) signaling. *Serinc5* enhances type I interferon (IFN) expression by activating NF- κ B signaling (Zeng et al. 2021). Additionally, NF- κ B signaling inhibits Sox9 transcriptional activity (Murakami, Lefebvre, and de Crombrughe 2000). Unexpectedly, however, NF- κ B inhibitor, BAY 11-7082, failed to rescue Sox9 function but further decreased *Col2a1* and *Acan* expression (Figure S6a). There are a few possibilities to explain these contradictions. One possibility is that *Serinc5* inhibits Sox9 function through an intracellular signaling pathway other than NF- κ B, as suggested by the lack of effect of BAY 11-7082 on Sox9 transcriptional activity (Figure S6b). Another possibility is that BAY 11-7082 suppresses *Col2a1* and *Acan* expression

independent of *Serinc5* and Sox9. Indeed, the role of NF- κ B in chondrocyte differentiation remains controversial. While some studies suggest that NF- κ B signaling promotes chondrogenesis (Caron et al. 2012; H. Kobayashi et al. 2016), others report that it inhibits Sox9 transcriptional activity (Murakami, Lefebvre, and de Crombrughe 2000). Therefore, further studies are needed to elucidate the mechanism by which *Serinc5* modulates Sox9 function.

Because serine plays essential roles in various biological processes, we cannot exclude the possibility that serine intake through *Serinc5* affects chondrocyte function. The palmitoylation of serine by serine palmitoyltransferase (SPT) is a key step

in ceramide synthesis (Perry 2002), and ceramide inhibits cellular proliferation but promotes apoptosis in chondrocytes (MacRae et al. 2006). Considering that hypertrophic chondrocytes stop proliferating and induce apoptosis, pre-hypertrophic chondrocytes need to increase their serine intake, and *Serinc5* supports this process. Therefore, it would be valuable to further investigate the roles of *Serinc5* in chondrocyte apoptosis.

Although we have revealed the function of *Serinc5* in chondrocyte differentiation in vitro, its in vivo significance in endochondral bone development remains unclear. Timilsina et al. generated *Serinc5*-deficient mice to examine the anti-retroviral effect of *Serinc5* in vivo but reported that *Serinc5*^{-/-} mice had no apparent developmental defects (Timilsina et al. 2020). We speculate that other serine proteins would compensate for the loss of *Serinc5* in chondrocytes. In line with this, scRNA-seq analysis showed ubiquitous expression of *Serinc1* and *Serinc3* in chondrocytes and osteoblasts (Figure 3d). However, the specific expression of *Serinc5* in pre-hypertrophic chondrocytes suggests a unique function not regulated by *Serinc1* and *Serinc3*. Notably, *Serinc3* showed no anti-retroviral effects, indicating functional differences between *Serinc3* and *Serinc5*. It would be interesting to examine the growth plate phenotype in *Serinc5* deficient mice.

4.3 | scRNA-Seq Analysis of Growth Plate Chondrocytes

In addition to pre-hypertrophic chondrocytes, scRNA-seq analysis of growth plate chondrocytes provided valuable insights. Superficial chondrocytes are also a minor cell population in growth plates. These cells give rise to articular cartilage, essential for shock absorption and smooth joint movement (Saito 2022). Despite their importance, the properties of superficial chondrocytes remain poorly understood.

From our scRNA-seq analysis, we identified a potential superficial chondrocyte cluster #0, specifically enriched with *Gdf5* (Figure 2). *Gdf5* is expressed at most epiphyseal ends of the growth plate, and lineage-tracing analysis using *Gdf5-Cre* mice revealed that *Gdf5*-expressing lineage cells give rise to articular cartilage (Koyama et al. 2008; Schwartz et al. 2016). These reports indicate that genes enriched in cluster #0 may play essential roles in articular cartilage development. Among the top 20 genes in this cluster include *Barx2* (Meech et al. 2005), *Osr1* (Gao et al. 2011), *Sfrp2* (Morello et al. 2008), *Creb5* (C.-H. Zhang et al. 2022), and *Lgr5* (C. Feng et al. 2019) which contribute to joint development (Figure S3). Notably, *Creb5* plays an essential role in synovial joint formation by directly regulating *Prg4* expression (C.-H. Zhang et al. 2022; C. H. Zhang et al. 2021). These findings suggest that other genes enriched in cluster #0 may play important roles in articular cartilage development. Our scRNA-seq datasets are valuable for identifying novel genes that regulate cartilage development.

In conclusion, we identified the specific expression of *Serinc5* in pre-hypertrophic chondrocytes and uncovered its role in chondrocyte differentiation. Our findings reveal the molecular basis of pre-hypertrophic bone formation, enhancing our understanding of the molecular mechanisms underlying endochondral bone formation.

Author Contributions

Kenji Hata, Kanta Wakamori, and Akane Yamamura performed the in vitro and in vivo experiments. Kenji Hata, Kanta Wakamori, and Riko Nishimura contributed to writing this paper. Sachi Ichiyama-Kobayashi, Yoshifumi Takahata, and Tomohiko Murakami performed molecular and biochemical experiments. Daisuke Okuzaki and Masaya Yamaguchi performed and analyzed the scRNA-seq data. Takashi Yamashiro and Riko Nishimura discussed and assessed the data. Kenji Hata and Riko Nishimura directed the project and interpreted the data.

Acknowledgments

We acknowledge the NGS core facility of the Genome Information Research Center at the Research Institute for Microbial Diseases of Osaka University for their support with the scRNA-seq analysis. This work was supported by JSPS KAKENHI, Grant Numbers JP23K24513 (K.H.), JP 21K19596 (K.H.), JP19K22708 (K.H.), JP 21H04841 (R.N.), JP 20K20475 (R.N.), and JP 16H06393 (R.N.).

Conflicts of Interest

The authors declare no conflicts of interest.

Data Availability Statement

The scRNA-seq data of *Col11a2-ZsGreen* mice and the ATAC-seq data of mesenchymal stem cells that support the findings of this study have been deposited in the NCBI Gene Expression Omnibus under the accession code GSE271633 (ATAC-seq) and GSE271634 (scRNA-seq).

References

- Amano, K., M. J. Densmore, and B. Lanske. 2015. "Conditional Deletion of Indian Hedgehog in Limb Mesenchyme Results in Complete Loss of Growth Plate Formation but Allows Mature Osteoblast Differentiation." *Journal of Bone and Mineral Research* 30, no. 12: 2262–2272. <https://doi.org/10.1002/jbmr.2582>.
- Buenrostro, J. D., B. Wu, H. Y. Chang, and W. J. Greenleaf. 2015. "ATAC-Seq: A Method for Assaying Chromatin Accessibility Genome-Wide." *Current Protocols in Molecular Biology* 109: 1–9. <https://doi.org/10.1002/0471142727.mb2129s109>.
- Caron, M. M. J., P. J. Emans, D. A. M. Surtel, et al. 2012. "Activation of NF-κB/p65 Facilitates Early Chondrogenic Differentiation During Endochondral Ossification." *PLoS One* 7, no. 3: e33467. <https://doi.org/10.1371/journal.pone.0033467>.
- Cooper, K. L., S. Oh, Y. Sung, R. R. Dasari, M. W. Kirschner, and C. J. Tabin. 2013. "Multiple Phases of Chondrocyte Enlargement Underlie Differences in Skeletal Proportions." *Nature* 495, no. 7441: 375–378. <https://doi.org/10.1038/nature11940>.
- Couasnay, G., M. B. Madel, J. Lim, B. Lee, and F. Elefteriou. 2021. "Sites of Cre-Recombinase Activity in Mouse Lines Targeting Skeletal Cells." *Journal of Bone and Mineral Research* 36, no. 9: 1661–1679. <https://doi.org/10.1002/jbmr.4415>.
- Feng, C., W. C. W. Chan, Y. Lam, et al. 2019. "Lgr5 and Col22a1 Mark Progenitor Cells in the Lineage Toward Juvenile Articular Chondrocytes." *Stem Cell Reports* 13, no. 4: 713–729. <https://doi.org/10.1016/j.stemcr.2019.08.006>.
- Feng, J., T. Liu, B. Qin, Y. Zhang, and X. S. Liu. 2012. "Identifying ChIP-Seq Enrichment Using MACS." *Nature Protocols* 7, no. 9: 1728–1740. <https://doi.org/10.1038/nprot.2012.101>.
- Gao, Y., Y. Lan, H. Liu, and R. Jiang. 2011. "The Zinc Finger Transcription Factors Osr1 and Osr2 Control Synovial Joint Formation." *Developmental Biology* 352, no. 1: 83–91. <https://doi.org/10.1016/j.ydbio.2011.01.018>.

- Gartland, A., J. Mechler, A. Mason-Savas, et al. 2005. "In Vitro Chondrocyte Differentiation Using Costochondral Chondrocytes as a Source of Primary Rat Chondrocyte Cultures: An Improved Isolation and Cryopreservation Method." *Bone* 37, no. 4: 530–544. <https://doi.org/10.1016/j.bone.2005.04.034>.
- Han, Y., and V. Lefebvre. 2008. "L-Sox5 and Sox6 Drive Expression of the Aggrecan Gene in Cartilage by Securing Binding of Sox9 to a Far-Upstream Enhancer." *Molecular and Cellular Biology* 28, no. 16: 4999–5013. <https://doi.org/10.1128/mcb.00695-08>.
- Hao, Y., S. Hao, E. Andersen-Nissen, et al. 2021. "Integrated Analysis of Multimodal Single-Cell Data." *Cell* 184, no. 13: 3573–3587.e29. <https://doi.org/10.1016/j.cell.2021.04.048>.
- Haseeb, A., R. Kc, M. Angelozzi, et al. 2021. "SOX9 Keeps Growth Plates and Articular Cartilage Healthy by Inhibiting Chondrocyte Dedifferentiation/Osteoblastic Redifferentiation." *Proceedings of the National Academy of Sciences* 118, no. 8: e2019152118. <https://doi.org/10.1073/pnas.2019152118>.
- Hata, K., R. Takashima, K. Amano, et al. 2013. "Arid5b Facilitates Chondrogenesis by Recruiting the Histone Demethylase Phf2 to Sox9-Regulated Genes." *Nature Communications* 4: 2850. <https://doi.org/10.1038/ncomms3850>.
- Hojo, H., S. Ohba, F. Yano, et al. 2012. "Gli1 Protein Participates in Hedgehog-Mediated Specification of Osteoblast Lineage During Endochondral Ossification." *Journal of Biological Chemistry* 287, no. 21: 17860–17869. <https://doi.org/10.1074/jbc.M112.347716>.
- Ichiyama-Kobayashi, S., K. Hata, K. Wakamori, et al. 2024. "Chromatin Profiling Identifies Chondrocyte-Specific Sox9 Enhancers Important for Skeletal Development." *JCI Insight* 9, no. 11: e175486. <https://doi.org/10.1172/jci.insight.175486>.
- Inada, M., Y. Wang, M. H. Byrne, et al. 2004. "Critical Roles for Collagenase-3 (Mmp13) in Development of Growth Plate Cartilage and in Endochondral Ossification." *Proceedings of the National Academy of Sciences* 101, no. 49: 17192–17197. <https://doi.org/10.1073/pnas.0407788101>.
- Inuzuka, M., M. Hayakawa, and T. Ingi. 2005. "Serinc, an Activity-Regulated Protein Family, Incorporates Serine Into Membrane Lipid Synthesis." *Journal of Biological Chemistry* 280, no. 42: 35776–35783. <https://doi.org/10.1074/jbc.M505712200>.
- Iwai, T., J. Murai, H. Yoshikawa, and N. Tsumaki. 2008. "Smad7 Inhibits Chondrocyte Differentiation at Multiple Steps During Endochondral Bone Formation and Down-Regulates p38 MAPK Pathways." *Journal of Biological Chemistry* 283, no. 40: 27154–27164. <https://doi.org/10.1074/jbc.M801175200>.
- Iwamoto, T., T. Nakamura, A. Doyle, et al. 2010. "Pannexin 3 Regulates Intracellular ATP/cAMP Levels and Promotes Chondrocyte Differentiation." *Journal of Biological Chemistry* 285, no. 24: 18948–18958. <https://doi.org/10.1074/jbc.M110.127027>.
- Knuth, C., E. Andres Sastre, N. Fahy, et al. 2019. "Collagen Type X Is Essential for Successful Mesenchymal Stem Cell-Mediated Cartilage Formation and Subsequent Endochondral Ossification." *European Cells and Materials* 38: 106–122. <https://doi.org/10.22203/eCM.v038a09>.
- Kobayashi, H., S. H. Chang, D. Mori, et al. 2016. "Biphasic Regulation of Chondrocytes by RelA Through Induction of Anti-Apoptotic and Catabolic Target Genes." *Nature Communications* 7, no. 1: 13336. <https://doi.org/10.1038/ncomms13336>.
- Kobayashi, T., U. Chung, E. Schipani, et al. 2002. "PTHrP and Indian Hedgehog Control Differentiation of Growth Plate Chondrocytes at Multiple Steps." *Development* 129, no. 12: 2977–2986.
- Koyama, E., Y. Shibukawa, M. Nagayama, et al. 2008. "A Distinct Cohort of Progenitor Cells Participates in Synovial Joint and Articular Cartilage Formation During Mouse Limb Skeletogenesis." *Developmental Biology* 316, no. 1: 62–73. <https://doi.org/10.1016/j.ydbio.2008.01.012>.
- Kronenberg, H. M. 2003. "Developmental Regulation of the Growth Plate." *Nature* 423, no. 6937: 332–336. <https://doi.org/10.1038/nature01657>.
- Langmead, B., and S. L. Salzberg. 2012. "Fast Gapped-Read Alignment With Bowtie 2." *Nature Methods* 9, no. 4: 357–359. <https://doi.org/10.1038/nmeth.1923>.
- Lauing, K. L., M. Cortes, M. S. Domowicz, J. G. Henry, A. T. Baria, and N. B. Schwartz. 2014. "Aggrecan Is Required for Growth Plate Cytoarchitecture and Differentiation." *Developmental Biology* 396, no. 2: 224–236. <https://doi.org/10.1016/j.ydbio.2014.10.005>.
- Lefebvre, V., G. Zhou, K. Mukhopadhyay, et al. 1996. "An 18-Base-Pair Sequence in the Mouse Pro α 1(II) Collagen Gene Is Sufficient for Expression in Cartilage and Binds Nuclear Proteins That Are Selectively Expressed in Chondrocytes." *Molecular and Cellular Biology* 16, no. 8: 4512–4523.
- Long, F., and D. M. Ornitz. 2013. "Development of the Endochondral Skeleton." *Cold Spring Harbor Perspectives in Biology* 5, no. 1: a008334. <https://doi.org/10.1101/cshperspect.a008334>.
- Long, J. T., A. Leinroth, Y. Liao, et al. 2022. "Hypertrophic Chondrocytes Serve as a Reservoir for Marrow-Associated Skeletal Stem and Progenitor Cells, Osteoblasts, and Adipocytes During Skeletal Development." *eLife* 11: e76932. <https://doi.org/10.7554/eLife.76932>.
- MacRae, V. E., T. Burdon, S. F. Ahmed, and C. Farquharson. 2006. "Ceramide Inhibition of Chondrocyte Proliferation and Bone Growth Is IGF-I Independent." *Journal of Endocrinology* 191, no. 2: 369–377. <https://doi.org/10.1677/joe.1.06958>.
- Madisen, L., T. A. Zwingman, S. M. Sunkin, et al. 2010. "A Robust and High-Throughput CRE Reporting and Characterization System for the Whole Mouse Brain." *Nature Neuroscience* 13, no. 1: 133–140. <https://doi.org/10.1038/nn.2467>.
- Mak, K. K., H. M. Kronenberg, P. T. Chuang, S. Mackem, and Y. Yang. 2008. "Indian Hedgehog Signals Independently of Pthrp to Promote Chondrocyte Hypertrophy." *Development* 135, no. 11: 1947–1956. <https://doi.org/10.1242/dev.018044>.
- Meech, R., D. B. Edelman, F. S. Jones, and H. P. Makarenkova. 2005. "The Homeobox Transcription Factor Barx2 Regulates Chondrogenesis During Limb Development." *Development* 132, no. 9: 2135–2146. <https://doi.org/10.1242/dev.01811>.
- Mizuhashi, K., M. Nagata, Y. Matsushita, W. Ono, and N. Ono. 2019. "Growth Plate Borderline Chondrocytes Behave as Transient Mesenchymal Precursor Cells." *Journal of Bone and Mineral Research* 34, no. 8: 1387–1392. <https://doi.org/10.1002/jbmr.3719>.
- Morello, R., T. K. Bertin, S. Schlaubitz, et al. 2008. "Brachy-Syndactyly Caused by Loss of Sfrp2 Function." *Journal of Cellular Physiology* 217, no. 1: 127–137. <https://doi.org/10.1002/jcp.21483>.
- Murakami, S., V. Lefebvre, and B. de Crombrughe. 2000. "Potent Inhibition of the Master Chondrogenic Factor Sox9 Gene by Interleukin-1 and Tumor Necrosis Factor- α ." *Journal of Biological Chemistry* 275, no. 5: 3687–3692. <https://doi.org/10.1074/jbc.275.5.3687>.
- Muramatsu, S., M. Wakabayashi, T. Ohno, et al. 2007. "Functional Gene Screening System Identified TRPV4 as a Regulator of Chondrogenic Differentiation." *Journal of Biological Chemistry* 282, no. 44: 32158–32167. <https://doi.org/10.1074/jbc.M706158200>.
- Olsen, B. R., A. M. Reginato, and W. Wang. 2000. "Bone Development." *Annual Review of Cell and Developmental Biology* 16: 191–220. <https://doi.org/10.1146/annurev.cellbio.16.1.191>.
- Ornitz, D. M., and L. Legeai-Mallet. 2017. "Achondroplasia: Development, Pathogenesis, and Therapy." *Developmental Dynamics* 246, no. 4: 291–309. <https://doi.org/10.1002/dvdy.24479>.
- Pacifici, M., E. Koyama, Y. Shibukawa, et al. 2006. "Cellular and Molecular Mechanisms of Synovial Joint and Articular Cartilage Formation." *Annals of the New York Academy of Sciences* 1068: 74–86. <https://doi.org/10.1196/annals.1346.010>.

Perry, D. K. 2002. "Serine Palmitoyltransferase: Role in Apoptotic De Novo Ceramide Synthesis and Other Stress Responses." *Biochimica et Biophysica Acta (BBA) - Molecular and Cell Biology of Lipids* 1585, no. 2–3: 146–152. [https://doi.org/10.1016/s1388-1981\(02\)00335-9](https://doi.org/10.1016/s1388-1981(02)00335-9).

Razzaque, M. S., D. W. Soegiarto, D. Chang, F. Long, and B. Lanske. 2005. "Conditional Deletion of Indian Hedgehog From Collagen Type 2 α 1-expressing Cells Results in Abnormal Endochondral Bone Formation." *The Journal of Pathology* 207, no. 4: 453–461. <https://doi.org/10.1002/path.1870>.

Rosa, A., A. Chande, S. Ziglio, et al. 2015. "HIV-1 Nef Promotes Infection by Excluding SERINC5 From Virion Incorporation." *Nature* 526, no. 7572: 212–217. <https://doi.org/10.1038/nature15399>.

Saito, T. 2022. "The Superficial Zone of Articular Cartilage." *Inflammation and Regeneration* 42, no. 1: 14. <https://doi.org/10.1186/s41232-022-00202-0>.

Shwartz, Y., S. Viukov, S. Krief, and E. Zelzer. 2016. "Joint Development Involves a Continuous Influx of Gdf5-Positive Cells." *Cell Reports* 15, no. 12: 2577–2587. <https://doi.org/10.1016/j.celrep.2016.05.055>.

St-Jacques, B., M. Hammerschmidt, and A. P. McMahon. 1999. "Indian Hedgehog Signaling Regulates Proliferation and Differentiation of Chondrocytes and Is Essential for Bone Formation." *Genes & Development* 13, no. 16: 2072–2086.

Stuart, T., and R. Satija. 2019. "Integrative Single-Cell Analysis." *Nature Reviews Genetics* 20, no. 5: 257–272. <https://doi.org/10.1038/s41576-019-0093-7>.

Takigawa, Y., K. Hata, S. Muramatsu, et al. 2010. "The Transcription Factor Znf219 Regulates Chondrocyte Differentiation by Assembling a Transcription Factory With Sox9." *Journal of Cell Science* 123, no. Pt 21: 3780–3788. <https://doi.org/10.1242/jcs.071373>.

Timilsina, U., S. Umthong, B. Lynch, A. Stablewski, and S. Stavrou. 2020. "SERINC5 Potently Restricts Retrovirus Infection In Vivo." *mBio* 11, no. 4: e00588-20. <https://doi.org/10.1128/mBio.00588-20>.

Tsumaki, N., T. Kimura, K. Tanaka, J. H. Kimura, T. Ochi, and Y. Yamada. 1998. "Modular Arrangement of Cartilage- and Neural Tissue-Specific cis-Elements in the Mouse α 2(XI) Collagen Promoter." *Journal of Biological Chemistry* 273, no. 36: 22861–22864.

Underhill, T. M., H. J. Dranse, and L. M. Hoffman. 2014. "Analysis of Chondrogenesis Using Micromass Cultures of Limb Mesenchyme." *Methods in Molecular Biology* 1130: 251–265. https://doi.org/10.1007/978-1-62703-989-5_19.

Usami, Y., Y. Wu, and H. G. Göttlinger. 2015. "SERINC3 and SERINC5 Restrict HIV-1 Infectivity and Are Counteracted by NEF." *Nature* 526, no. 7572: 218–223. <https://doi.org/10.1038/nature15400>.

Yang, L., K. Y. Tsang, H. C. Tang, D. Chan, and K. S. E. Cheah. 2014. "Hypertrophic Chondrocytes Can Become Osteoblasts and Osteocytes in Endochondral Bone Formation." *Proceedings of the National Academy of Sciences* 111, no. 33: 12097–12102. <https://doi.org/10.1073/pnas.1302703111>.

Yoshida, M., K. Hata, R. Takashima, et al. 2015. "The Transcription Factor Foxc1 Is Necessary for Ihh-Gli2-regulated Endochondral Ossification." *Nature Communications* 6: 6653. <https://doi.org/10.1038/ncomms7653>.

Zeng, C., A. A. Waheed, T. Li, et al. 2021. "SERINC Proteins Potentiate Antiviral Type I IFN Production and Proinflammatory Signaling Pathways." *Science Signaling* 14, no. 700: eabc7611. <https://doi.org/10.1126/scisignal.abc7611>.

Zhang, C.-H., Y. Gao, H.-H. Hung, Z. Zhuo, A. J. Grodzinsky, and A. B. Lassar. 2022. "Creb5 Coordinates Synovial Joint Formation With the Genesis of Articular Cartilage." *Nature Communications* 13, no. 1: 7295. <https://doi.org/10.1038/s41467-022-35010-0>.

Zhang, C. H., Y. Gao, U. Jadhav, et al. 2021. "Creb5 Establishes the Competence for Prg4 Expression in Articular Cartilage."

Communications Biology 4, no. 1: 332. <https://doi.org/10.1038/s42003-021-01857-0>.

Supporting Information

Additional supporting information can be found online in the Supporting Information section.